Title

Miniature optical coherence tomography-ultrasound probe for automatically coregistered three-dimensional intracoronary imaging with real-time display

Journal

Journal of Biomedical Optics, 18(10)

ISSN

1083-3668

Authors

Li, Jiawen

Ma, Teng

Jing, Joseph

et al.

Publication Date

2013-10-01

DOI

10.1117/1.jbo.18.10.100502

Peer reviewed

Journal of Biomedical Optics

SPIEDigitalLibrary.org/jbo

Miniature optical coherence tomography-ultrasound probe for automatically coregistered three-dimensional intracoronary imaging with real-time display

Jiawen Li
Teng Ma
Joseph Jing
Jun Zhang
Pranav M. Patel
K. Kirk Shung
Qifa Zhou
Zhongping Chen

SPIE

Miniature optical coherence tomography-ultrasound probe for automatically coregistered three-dimensional intracoronary imaging with real-time display

Jiawen Li,[a,c,e*] Teng Ma,[b*] Joseph Jing,[a,c] Jun Zhang,[c] Pranav M. Patel,[d,e] K. Kirk Shung,[b] Qifa Zhou,[b] and Zhongping Chen[a,c,e]

[a]University of California, Irvine, Department of Biomedical Engineering, Irvine, California 92612
[b]University of Southern California, NIH Ultrasonic Transducer Resource Center, Los Angeles, California 90089
[c]University of California, Irvine, Beckman Laser Institute, Irvine, California 92612
[d]University of California, Irvine, Division of Cardiology, Irvine, California 92868
[e]University of California, Irvine, The Edwards Lifesciences Center for Advanced Cardiovascular Technology, Irvine, California 92617

Abstract. We have developed a novel miniature integrated optical coherence tomography (OCT)-intravascular ultrasound (IVUS) probe, with a 1.5-mm-long rigid part and 0.9-mm outer diameter, for real-time intracoronary imaging of atherosclerotic plaques and guiding of interventional procedures. By placing the OCT ball lens and IVUS transducer back-to-back at the same axial position, this probe can provide automatically coregistered, coaxial OCT-IVUS imaging. To demonstrate its real-time capability, three-dimensional OCT-IVUS imaging of a pig's coronary artery displaying in polar coordinates, as well as images of three major types of atherosclerotic plaques in human cadaver coronary segments, were obtained using this probe and our upgraded system. Histology validation is also presented.

 [DOI: 10.1117/1.JBO.18.10.100502]

Keywords: intravascular optical coherence tomography; ultrasound; atherosclerosis; online coregistration.

Paper 130525LR received Jul. 24, 2013; revised manuscript received Sep. 5, 2013; accepted for publication Sep. 16, 2013; published online Oct. 21, 2013.

Each year, more than 20 million patients worldwide with coronary artery disease (CAD) experience acute coronary syndrome (ACS).[1] Thirty-four percent of these individuals die from CAD complications in a given year.[2] ACS is caused by the accumulation of vulnerable atherosclerotic plaques within coronary artery walls. Since most CAD occurs at a length scale of 2 to 2000 μm, it is essential to have high-resolution and deep-penetration imaging technology on this scale to visualize vascular plaque elements in the coronary artery wall. Currently, only intravascular ultrasound (IVUS) and intravascular optical coherence tomography (OCT) are able to provide cross-sectional real-time visualization of the coronary artery wall. However, due to intrinsic limitations of resolution and penetration depth, respectively, neither IVUS nor OCT alone is able to accurately assess plaque characteristics.[3–6] Combined use of IVUS and OCT holds the potential of combining the strengths of both imaging modalities and improving the diagnostic accuracy of plaque vulnerability.[4,6,7] Thus, fusion of these two complimentary medical image modalities[4,5,8] is clinically important in providing improved diagnostic information.

There have been several reports demonstrating the feasibility and potential effectiveness of the combined use of OCT and IVUS in different clinical settings for vulnerable plaques recognition.[4,7] Nevertheless, there are major limitations to previous approaches using offline fusion of OCT and IVUS;[4,7] prior to fusion, matching OCT and IVUS lesions based on manual identification of landmarks, such as side-branches or calcification, is required. The matching procedures are not only tediously slow but also may lead to inaccurate coregistration, because lumens constantly change shape and the images acquired may not be identical at different points in time within each cardiac cycle. They cannot be used for real-time display either, severely limiting clinical utility for guiding interventions during a catheterization procedure. The ability to fully integrate OCT and IVUS capabilities into a single imaging system for *in vivo* assessment of plaques[6,7] will help overcome these limitations. Fully integrated techniques are also less time consuming, less traumatic, provide less radiation exposure, use fewer contrast agents, and provide more accurate imaging capabilities with the potential for a real-time fusion image display.

In preliminary research, our group first developed an integrated OCT-IVUS system and imaging probe.[9–11] Independently, Li et al.[12] designed a similar hybrid OCT-IVUS system and used it for *in vitro* human cadaver imaging. Although Li's design enables colocalized imaging, the side-by-side design prevents coaxial IVUS-OCT imaging and true image coregistration. Recently, we reported the safe and successful *in vivo* imaging of plaques in rabbits and coronary arteries in a swine, using a miniature probe design.[10] However, one limitation of the previously employed miniature probe[10] was its difficulty to coregister data in real time, due to the offset between the OCT prism and IVUS transducer.

In this paper, we present a novel design for a miniature integrated probe that overcomes this limitation. The new design uses back-to-back OCT-IVUS probes to facilitate imaging at the same regions of interest simultaneously. This catheter enables real-time imaging and display of coregistered OCT-IVUS images for identifying vulnerable plaques and guiding coronary intervention, which better fits clinical needs compared to the previous probe design with an offline fusion method. In addition, our current integrated probe design has a rigid-part size similar to the clinically used IVUS or OCT probe, has a clinically acceptable outer diameter (OD), and does not sacrifice image quality. The reduction in probe size is essential to enable safer OCT-IVUS delivery for clinical applications. We report the

*Both authors contributed equally to this work.

Address all correspondence to: Zhongping Chen, University of California, Irvine, Beckman Laser Institute, 1002 Health Sciences Road East, Irvine, California 92612. Tel: 949-824-1247; Fax: 949-824-8413; E-mail: z2chen@uci.edu

0091-3286/2013/$25.00 © 2013 SPIE

first demonstration of real-time three-dimensional (3-D) imaging and display of coregistered OCT-IVUS images in polar coordinates. The 3-D intracoronary imaging of familial hypercholesterolemic (FH) swine[13] is shown herein. Images of three major types of atherosclerotic plaques in human cadaver coronary segments further demonstrate the imaging capability of this novel probe.

With the guidance of visible light from the OCT subprobe, a back-to-back, coregistered OCT-IVUS probe [Figs. 1(b) and 1(c)] was made by carefully aligning an OCT subprobe with an IVUS subprobe, while confirming that the light beam and sound wave exit at the same axial position, but 180 deg apart. This integrated probe provides automatically coregistered and coaxial fusion imaging. The combined probe was then inserted into a customized probe cap (a stainless steel tube with two windows; OD: 0.9 mm; length: 1.5 mm). Following the probe cap, we used a double wrapped torque coil to encompass the fiber and electrical wire, giving the probe adequate flexibility and torque control. During experiments, the probe was inserted into a sheath. Water was filled in the sheath to facilitate ultrasound imaging.

We used a $0.4 \times 0.4 \times 0.3$ mm, 45-MHz (1-x)[Pb(Mg1/3Nb2/3)O3]-x[PbTiO3] (PMN-PT) single-element transducer for our IVUS subprobe, which is thinner than in previous designs.[9,10] The functional element was lapped to a thickness of only 300 μm before it was mechanically diced into 0.4×0.4 mm square shape. The center core of a coaxial cable was connected to the side of the backing layer and covered by epoxy to insulate from the front electrode without increasing the thickness of the transducer. For the OCT subprobe, we chose a ball-lens design, which enables less insertion loss and stronger interfaces[14] than the traditional Gradient-index (GRIN) lens design.[12] Ball lenses also have the potential to be manufactured in large quantities while maintaining constant performance. A single-mode fiber was fusion-spliced to a fiber spacer (cladding OD: 0.125 mm; reflective index: 1.457) using a splicing workstation. Then, a ball with a 560-μm-long fiber spacer[14] was created at the distal end of the fiber spacer using the splicing workstation. This ball lens can generate a beam focusing at ~1 mm from the ball surface. Next, the lens was mechanically polished until the angle between the polished surface and optical fiber was <37 deg. The ball lens was later inserted into a sealed polyimide tube, isolating the ball lens from the water in the sheath and maintaining an air-fiber interface to ensure that the total internal reflection was generated at the polished surface.

All imaging was performed using the integrated OCT-IVUS system[10] [Fig. 1(a)] at 1000 pixels per frame, 10 frames per second, 2.5 mm/s pull-back speed. Current system speed is limited by the ultrasound subsystem speed. However, it is possible to improve the imaging pull-back speed to 25 mm/s,[15] the commercial OCT system speed. The coregistered OCT-IVUS polar domain image pairs were displayed in real time, by rotating OCT images 180 deg to match IVUS images' orientation and converting them from Cartesian coordinates to polar coordinates, using a commercial graphical processing unit. This is the first report of the capability to display real-time OCT-IVUS imaging in polar coordinates.

We used coronary arteries from swine and human cadavers to demonstrate the imaging capabilities of this probe. FH swine is an ideal atherosclerotic animal model for intravascular imaging,[13] since lesions formed in FH swine closely mimic advanced human atherosclerosis. Human coronary arteries, which were up to 3 days postmortem and fixed with formalin, were also used for imaging. Plaques were imaged with this OCT-IVUS integrated system in phosphate-buffered saline at room temperature. After imaging, each coronary artery segment was sectioned for histology analysis.

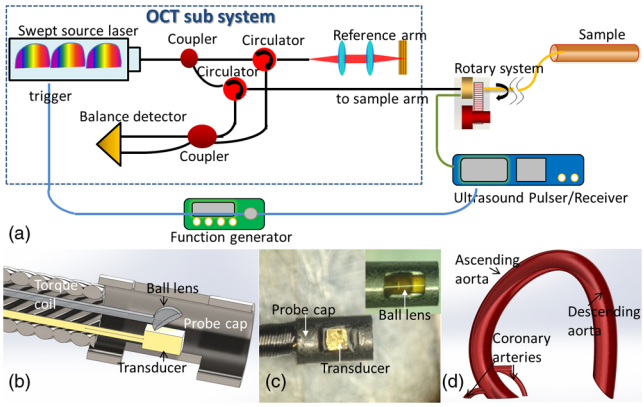

Fig. 1 (a) Schematic of the integrated imaging system. The dashed box illustrates the optical coherence tomography (OCT) subsystem, a swept source OCT system. Black lines, a green line, and a blue line denote the optical path, the ultrasound path, and the electrical trigger signal, respectively (original schematic published in JACC supplementary information). (b) Schematic of back-to-back OCT-intravascular ultrasound (IVUS) probe. (c) Photo of back-to-back probe, showing the transducer. Insert: photo showing the OCT subprobe. (d) Schematic of cardiovascular system.

A typical cardiovascular system is shown in Fig. 1(d). The system includes several sharp turns: from the descending aorta to ascending aorta, there is a curve of >180 deg. Furthermore, the right (or left) coronary artery and ascending aorta are normally 80 to 90 deg angularly spaced. This curvy structure demands a probe with high flexibility, small diameter, and short length of the rigid part to provide safe access to the coronary arteries. In previously reported probe designs,[9–12] either the probe's OD is too large or the rigid part is too long, both of which potentially reduce the safety of catheter interventions. The probe previously reported by our group has a 0.7-mm OD but a rigid part as long as ~3.5 mm,[10] while the probe reported by Li[12] has a 2.5-mm-long rigid part, but an OD as large as 1.0 mm. The back-to-back ball-lens design probe reported here minimizes the probe's rigid part to 1.5 mm length, which is the same size as clinically used IVUS or OCT rigid parts, while maintaining an OD of 0.9 mm. The reduction of probe size is a significant improvement, which allows for safer access to the coronary artery system. Using available space more efficiently than previous designs, we further reduce probe size without reducing the size of optical lenses, hence maintaining image quality. Standard pulse-echo testing was performed to evaluate the thinner (300 μm) IVUS transducer's performance. The center frequency of the IVUS transducer was found to be 45 MHz, exhibiting a −6 dB fractional bandwidth of 40%. Thus, the IVUS transducer demonstrated satisfactory performance compared to those in previously published reports.[9,10]

Representative OCT-IVUS image pairs of coronary artery segments with calcified plaques and a lipid-fibrous plaque are shown in Figs. 2(Ia) to 2(IId) and Figs. 2(IIIa) to 2(IIId), respectively. Sharp boundaries in OCT [Figs. 2(Ia) and 2(IIa) arrows] and acoustic shadows in IVUS [Figs. 2(Ib) and 2(IIb) arrows] demonstrate the locations of calcified plaques, where IVUS is superior in detecting deep calcification [Fig. 2(II) arrows] and OCT is superior in depicting superficial calcification with well-defined boundaries [Fig. 2(I) arrows]. The

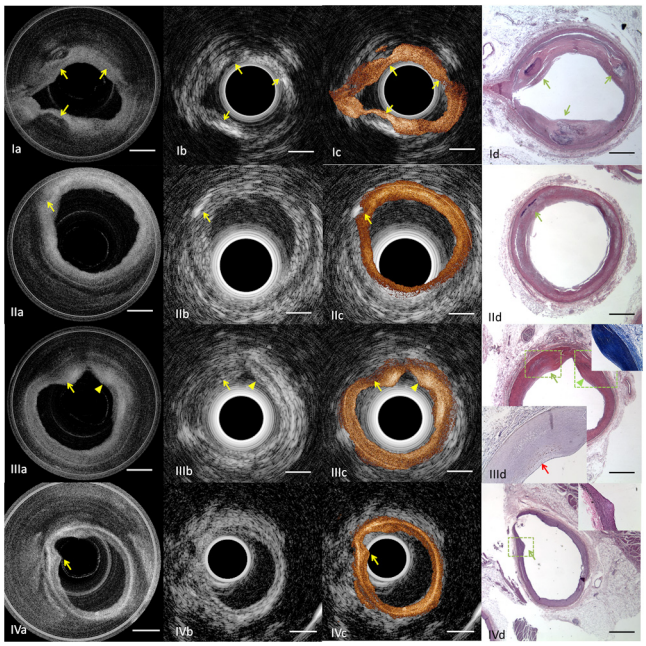

Fig. 2 Top row: Images of calcified plaques. (Ia) OCT, (Ib) IVUS, and (Ic) merged OCT-IVUS cross-sectional images of a human coronary artery with calcified plaque. (Id) Corresponding H&E histology. Second row: Images of coronary artery with deep calcification, indicating that OCT lacks the capability to clearly visualize deep calcification. (IIa) OCT, (IIb) IVUS, and (IIc) merged OCT-IVUS cross-sectional images of human coronary artery with a calcified plaque. (IId) Corresponding H&E histology. Third row: Images of necrotic plaque and fibrous plaque. (IIIa) OCT, (IIIb) IVUS, and (IIIc) merged OCT-IVUS cross-sectional images of human coronary artery with necrotic plaque and fibrous plaque. (IIId) Corresponding histology. Arrow: necrotic plaque. Arrow head: fibrous plaque. Top inset: highly magnified image of the top box region, Trichrome stain. Inset image confirms the existence of fibrous plaque. Bottom inset: Highly magnified image of the bottom box region, CD 68 stain. Red arrow points to the positive CD 68 stain regions, which confirm the existence of macrophages. Bottom row: Images of familial hypercholesterolemic (FH) swine coronary artery with intimal hyperplasia. Still frame from 35:00 s of (Video 1, MPEG, 10.0 MB) [URL: http://dx.doi.org/10.1117/1.JBO.18.10.100502.1]. (IVa) OCT, (IVb) IVUS, and (IVc) merged OCT-IVUS of FH swine coronary artery with intimal hyperplasia. (IVd) Corresponding H&E histology. Inset: Highly magnified image of Elastic stain. Scale bar: 1 mm.

signal-high region in the OCT image [Fig. 2(IIIa) arrowhead] demonstrates the location of a fibrous plaque. The signal-low region overlaying diffused boundary in the OCT image [Fig. 2(IIIa) arrow] demonstrates the location of a necrotic plaque. These two plaque types, fibrous and lipid, are difficult to be differentiated by corresponding IVUS image, due to its low soft-tissue contrast [Fig. 2(IIIb) arrow and arrowhead]. Histology photos validate the plaque type classification by OCT-IVUS images. Video 1 of an FH swine supports the real-time 3-D imaging and automatically coregistered display capability of this probe design. We scanned a ~5-cm-long segment of the swine coronary artery to investigate the existence and location of plaques; the existence of an intimal hyperplasia is shown in Figs. 2(IVa) to 2(IVd) (arrows).

In summary, we have developed a novel miniature probe for automatically coregistered OCT-IVUS imaging. With our probe and system, 3-D OCT-IVUS imaging with online real-time fusion is achieved. Real-time 3-D imaging of an FH swine coronary artery demonstrated the coregistered nature of this probe and the polar image display capability of this system. Human plaques' morphologic characteristics were also clearly imaged. This design enables real-time *in situ* characterization of plaques and guiding of coronary intervention, which is essential in translating this technology from bench to clinical application.

Acknowledgments

This work was supported by the National Institutes of Health under grants R01EB-10090, R01HL-105215, R01EY-021519, P41-EB002182, P41EB-015890. We acknowledge Ms. Leacky Liaw, Ms. Linda Li, Mr. Hataka Minami, and Mr. Andrew Heidari for their assistance in histology and Solidwork drawing. The authors wish to thank individuals who donated their bodies and tissues for the advancement of education and research. Dr. Zhongping Chen has a financial interest in OCT Medical Inc., which, however, does not support this work.

References

1. WHO, "The world health report 2002—Reducing risks, promoting healthy life," World health organization, Geneva , Switzerland (2002).
2. V. L. Roger et al., "Heart disease and stroke statistics—2011 update: a report from the American Heart Assoctiation," *Circulation* **123**(4), 18–209 (2011).
3. T. Thim et al., "Unreliable assessment of necrotic core by virtual histology intravascular ultrasound in porcine coronary artery disease," *Circ. Cardiovasc. Imaging* **3**(4), 384–391 (2010).
4. T. Sawada et al., "Feasibility of combined use of intravascular ultrasound radiofrequency data analysis and optical coherence tomography for detecting thin-cap fibroatheroma," *Eur. Heart J.* **29**(9), 1136–1146 (2008).
5. M. Kawasaki et al., "Diagnostic accuracy of optical coherence tomography and integrated backscatter intravascular ultrasound images for tissue characterization of human coronary plaques," *J. Am. Coll. Cardiol.* **48**(1), 81–88 (2006).
6. R. Puri, M. I. Worthley, and S. J. Nicholls, "Intravascular imaging of vulnerable coronary plaque: current and future concepts," *Nat. Rev. Cardiol.* **8**(3), 131–139 (2011).
7. L. Räber et al., "Offline fusion of co-registered intravascular ultrasound and frequency domain optical coherence tomography images for the analysis of human atherosclerotic plaques," *EuroIntervention* **8**(1), 98–108 (2012).
8. J. Rieber et al., "Diagnostic accuracy of optical coherence tomography and intravascular ultrasound for the detection and characterization of atherosclerotic plaque composition in ex-vivo coronary specimens: a comparison with histology," *Coron Artery Dis.* **17**(5), 425–430 (2006).
9. J. Yin et al., "Integrated intravascular optical coherence tomography ultrasound imaging system," *J. Biomed. Opt.* **15**(1), 010512 (2010).
10. J. Yin et al., "Novel combined miniature optical coherence tomography ultrasound probe for in vivo intravascular imaging," *J. Biomed. Opt.* **16**(6), 060505 (2011).
11. X. Li et al., "High-resolution coregistered intravascular imaging with integrated ultrasound and optical coherence tomography probe," *Appl. Phys. Lett.* **97**(13), 133702 (2010).
12. B. H. Li et al., "Hybrid intravascular ultrasound and optical coherence tomography catheter for imaging of coronary atherosclerosis," *Catheter. Cardiovasc. Interv.* **81**(3), 494–507 (2013).
13. D. Hamamdzic and R. L. Wilensky, "Porcine models of accelerated coronary atherosclerosis: role of diabetes mellitus and hypercholesterolemia," *J. Diabetes Res.* **2013**, 761415 (2013).
14. Y. Mao, S. Chang, and C. Flueraru, "Fiber lenses for ultra-small probes used in optical coherent tomography," *J. Biomed. Sci. Eng.* **3**(1), 27–34 (2010).
15. X. Li et al., "Integrated IVUS-OCT imaging for atherosclerotic plaque characterization," *IEEE J. Sel. Topics Quantum Electron.* **20**(2), 1–8 (2014).